Hydrometallurgy 173 (2017) 134–148

Contents lists available at ScienceDirect

Hydrometallurgy

journal homepage: www.elsevier.com/locate/hydromet

Dynamic multi-objective optimization arising in iron precipitation of zinc hydrometallurgy

Jie Han, Chunhua Yang*, Xiaojun Zhou, Weihua Gui

School of Information Science and Engineering, Central South University, Changsha 410083, PR China

ARTICLE INFO

Keywords:
Dynamic multi-objective optimization
Discretization method
State transition algorithm
Iron precipitation

ABSTRACT

The additions of oxygen and zinc oxide for the goethite process determine the cost and efficiency of the iron precipitation process. As the two production targets (cost and efficiency) are conflicting and the chemical reaction is a continuous process that changes over time, the amounts of additive need to be dynamically optimized to satisfy the requirement of industrial application. In this paper, a discretization method based on control variables and control intervals is proposed to transform the dynamic optimization problem to a nonlinear mathematical programming problem. Then, a multi-objective optimization approach based on the state transition algorithm and constrained nondominated sorting is proposed to find the Pareto optimal solutions. Finally, an evaluation mechanism is proposed to obtain the best solution for industrial applications. The results from a series of simulation experiments show the effectiveness of the proposed approach, e.g. the daily average additions of oxygen and zinc oxide are decreased by 778.0854 m^3 and 4.9013 t, respectively.

1. Introduction

Currently, zinc hydrometallurgy industry produces approximately 80% of zinc production worldwide (Balarini et al., 2008). The process of atmospheric direct leaching of zinc concentrate under oxygen-rich conditions involves five steps: roasting, calcine leaching, solution purification, electrowinning, and melting (Takala, 1999; Zhang et al., 2016). Since iron contained in zinc concentrates is the oxygen carrier which can improve the reaction rate in leaching, the leaching solution has high concentration of iron, especially in the ferrous form. However, iron can significantly disturb the solution purification and the electrowinning of zinc by decreasing current efficiency. Therefore, appropriate control of the iron precipitation step is important to the zinc hydrometallurgy process.

In zinc hydrometallurgy, iron can be mainly precipitated as goethite (FeOOH) (Pappu et al., 2006), jarosite ($KFe_3(SO_4)_2(OH)_6$) (Pradel et al., 1993), hematite (Fe_2O_3) (Ismael and Carvalho, 2003), and paragoethite ($Fe_2O_5 \cdot 9H_2O$) (Güler and Seyrankaya, 2016; Loan et al., 2006). The goethite process is always considered as the most common way to remove iron because it has better filterability, higher purity, and larger crystal size (Chang et al., 2010). In the goethite process, the ferrous iron is oxidized to the ferric iron by feeding oxygen into the zinc sulfate solution, and the ferric iron is hydrolyzed to form the goethite polymer precipitate. Moreover, in order to keep the acid-base equilibrium of the goethite process, zinc oxide needs to be added in the reaction solution (Na et al., 2016). The details of this process can be simply described by following chemical equations (Xie et al., 2015a).

$$\text{Oxidation reaction: } 4Fe^{2+} + 4H^+ + O_2 \rightarrow 4Fe^{3+} + 2H_2O, \quad (1)$$

$$\text{Hydrolysis reaction: } Fe^{3+} + 2H_2O \rightarrow FeOOH + 3H^+, \quad (2)$$

$$\text{Neutralization reaction: } 2H^+ + ZnO \rightarrow Zn^{2+} + H_2O, \quad (3)$$

where the nature of underlying microscopic phenomena is chaotic and complicated (control of the iron precipitation process is difficult). On the one hand, the reaction condition, including the total iron concentration and the pH value, must be within the strict limits of technical requirements. For example, if the pH value is too high, the precipitations of other impurities will be formed, such as $Cu(OH)_2$; whereas if the pH value is too low, the precipitate will be redissolved. Because the iron concentration and pH value can be adjusted by O_2 and ZnO, the reasonable control of the amounts of additive is very important to the iron precipitation process.

On the other hand, the cost and the efficiency (two production targets) of the iron precipitation process can also be adjusted by the additions of oxygen and zinc oxide. For instance, if the amounts of additive are too high, it will lead to huge economic loss. On the contrary, if the amounts of additive are too low, the efficiency of the iron precipitation (which is a performance metric of the process and can be defined as the percentage of removed ferrous iron) will be reduced. This is due to the fact that insufficient oxygen will result in excessive outlet

* Corresponding author.
E-mail addresses: hanjie@csu.edu.cn (J. Han), ychh@csu.edu.cn (C. Yang), michael.x.zhou@csu.edu.cn (X. Zhou), gwh@csu.edu.cn (W. Gui).

http://dx.doi.org/10.1016/j.hydromet.2017.08.007
Received 2 March 2017; Received in revised form 1 July 2017; Accepted 6 August 2017
Available online 12 August 2017
0304-386X/

ferrous iron while insufficient zinc oxide will cause precipitate to dissolve. Thus, it is important to find the Pareto optimal solution to represent the trade-off between the two production objectives when determining the amounts of additive. Moreover, since the chemical reaction in the iron precipitation process is a continuous process that changes over time (follows first-order kinetics), the control of the amounts of additive turns out to be a dynamic multi-objective optimization problem.

To the authors' best knowledge, there exists no effective method to consider both cost and efficiency for the iron precipitation process. One recent paper, (Xie et al., 2017) only investigated the cost of the goethite process with dynamic modeling and optimal control (only optimizes the consumption of oxygen and zinc oxide). Note that currently the dynamic multi-objective method has attracted the attention of many researchers and has been applied to industrial applications (Chen et al., 2015; Farina et al., 2004; Helbig and Engelbrecht, 2013). Kong et al. (2013) proposed a hybrid evolutionary multi-objective optimization strategy for the dynamic power supply problem in magnesia grain manufacturing. Bayat et al. (2014) used the dynamic multi-objective optimization method to deal with the control of industrial radial-flow fixed-bed reactor of heavy paraffin dehydrogenation. Soroudi and Afrasiab (2012) adopted the binary PSO-based dynamic multi-objective model to optimize distributed generation planning under uncertainty. Riascos and Pinto (2004) proposed a simultaneous optimization approach using orthogonal collocation to solve the optimal control problem in bioreactors.

The dynamic multi-objective optimization of the iron precipitation process is a challenging problem, because its model not only has nonconvex functions (including differential equations) but also is a highly nonlinear, multidimensional, and multimodal problem with many constraints (Na et al., 2016). In this paper, a dynamic multi-objective optimization method based on a global optimization algorithm is proposed to optimize the process of iron precipitation by goethite.

The major contributions and novelty of this paper are briefly summarized as follows.

(1) A dynamic optimization model for iron precipitation by goethite is established, which not only minimizes the cost but also maximizes the efficiency of the iron precipitation process;
(2) A discretization method based on control variables and control intervals is proposed to transform the dynamic optimization problem to a nonlinear mathematical programming problem, and the state transition algorithm (STA) based on constrained nondominated sorting is introduced to solve the multi-objective optimization problem;
(3) An evaluation mechanism based on the concentration of ions and their trends is proposed to select the best result for industrial applications;
(4) By comparing the simulation results with those obtained from manual control, the effectiveness of the proposed method is presented.

2. Materials and method

2.1. Process description

The iron precipitation process is an important part of the atmospheric direct leaching of zinc concentrates, and the goethite process is used to validate and test the effectiveness of optimization and control strategy. The flow diagram of the goethite process in a certain zinc hydrometallurgy plant in China is shown in Fig. 1. The leaching solution entering the reactors is composed of various impurities (iron content is the highest). Iron is precipitated in four connected continuous stirred tank reactors (300 m^3). Oxygen and zinc oxide are fed into the reactor to maintain the concentration of outlet solution within the desired limits. After the precipitation reaction is finished, the outlet solution from the last reactor is sent to a overflow tank, meanwhile the precipitate is separated from the purified solution by thickener. The solution from the top of the thickener is pumped to the other process for further treatment, while a portion of the precipitate from the bottom of the thickener is recycled to the first reactor. The remaining precipitate is finally sent to the filter press to produce goethite.

During the goethite process, the amounts of zinc oxide and oxygen added to the reactors are adjusted according to the manufacturing-condition and human-experience. Note that the latest specifications of the influent and the effluent in the goethite process (from the first reactor (#1) to the last reactor (#4)) are shown in Table 1.

2.2. Dynamic multi-objective optimization model

A dynamic multi-objective optimization model for the goethite process is established in this subsection. By optimizing the amounts of additive in each reactor, we are able to reduce the cost of additives as low as possible and maintain the efficiency of the iron precipitation process as high as possible, where all the technical requirements of Table 1 are met.

2.2.1. Assumptions

The following assumptions are considered in the problem formulation:

(1) The temperature and agitation rates in each reactor vary little, so they are considered to be constant.
(2) In the normal production process, the flow rate of influent and underflow do not fluctuate significantly and are therefore considered to be constant.

2.2.2. Objective functions

During the goethite process, the concentration of the ferrous iron, ferric iron, and hydrogen ion must be maintained to a desired level by adding zinc oxide and oxygen. So the state variables consist of the concentration of Fe^{2+}, Fe^{3+} and H^+ in $\#i(i = 1,2,3,4)$ reactor, which are described as $\mathbf{c}^i = [c_1^i, c_2^i, c_3^i]^T$. The inlet concentration of Fe^{2+}, Fe^{3+} and H^+ in the $\#i$ reactor are defined as $\mathbf{c_0^i} = [c_{0,1}^i, c_{0,2}^i, c_{0,3}^i]^T$. The control variables in $\#i$ reactor are the rate of the additions of oxygen and zinc oxide, which can be defined as $\mathbf{u}^i = [u_1^i, u_2^i]$. Thus, the objective functions of the dynamic multi-objective optimization model are defined as

$$\begin{aligned} \min \quad & J_1 = \int_0^{T_f} (p_1{}^*u_1(t) + p_2{}^*u_2(t))dt \\ \max \quad & J_2 = \frac{c_{0,1}^1(0) - c_1^4(T_f)}{c_{0,1}^1}, \end{aligned} \tag{4}$$

where $u_1(t) = \sum_{i=1}^4 u_1^i(t)$ and $u_2(t) = \sum_{i=1}^4 u_2^i(t)$. J_1 denotes the total cost of oxygen and zinc oxide, while J_2 refers the efficiency of iron precipitation (the percentage of the removed ferrous iron). p_1 and p_2 are the price of oxygen and zinc oxide, respectively. T_f represents the time of solution from the #1 reactor to #4 reactor, $T_f = 4V/(F + F_u)$, where F and F_u are the flow rate of the leaching solution and the underflow, respectively. V denotes the volume which is the same for all reactors.

It is worth mentioning that the solution will flow out from #4 reactor after the reaction time T_f. In this paper, the efficiency of the iron precipitation process is defined by the inlet concentration of ferrous iron in #1 reactor at time 0 and the outlet concentration of ferrous iron in #4 reactor at time T_f.

2.2.3. The dynamic state variable model

As shown in Eqs. (1) to (3), there are three major chemical reactions in the goethite process. Based on the theory of first order kinetics, the reactions in four reactors can be analyzed as follows.

Firstly, since the copper ion in oxidation reaction has a catalytic effect, the reaction in Eq. (1) can be divided into two sub-step reactions

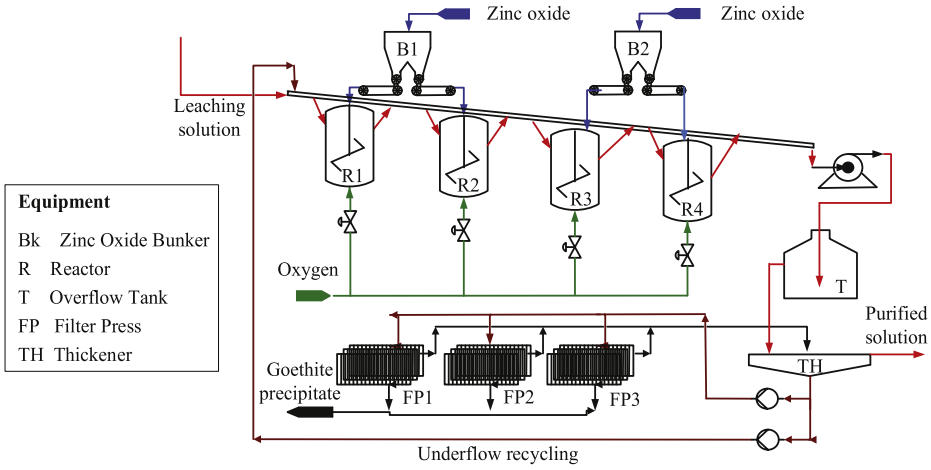

Fig. 1. Flow diagram of the goethite process.

Table 1
The desired specifications of the influent and the effluent in the goethite process.

Parameter	Unit	Influent	#1Effluent	#2Effluent	#3Effluent	#4Effluent
Flow rate of leaching solution	m^3/h	80–200	–	–	–	–
Flow rate of underflow	m^3/h	40–60	–	–	–	–
Temperature	K	353	–	–	–	–
Cu^{2+}	g/L	0.9–3	–	–	–	–
pH	–	2–2.5	2.7–3.5	2.7–3.5	2.7–3.5	2.7–3.5
Fe^{3+}	g/L	1–2	≤2	≤2	≤2	≤2
Fe^{2+}	g/L	9–15	6–8	2.5–5	1–2	0.3 ≤ 0.8

(Stumm and Lee, 1961), which are shown as follows:

$$Fe^{2+} + Cu^{2+} \rightarrow Fe^{3+} + Cu^{+} \quad (5\text{-a})$$

$$4Cu^{+} + O_2 + 4H^{+} \rightarrow 4Cu^{2+} + 2H_2O \quad (5\text{-b})$$

According to the historical measurement data obtained from the zinc hydrometallurgy plant (Xie et al., 2017), the ferrous iron concentration and oxygen concentration in four reactors can be shown in Table 2.

Based on the principle of mass conservation in oxidation reaction, 4 mol of ferrous iron will react with 1 mol of oxygen. In #1 reactor, the concentration of oxygen is much lower than that of ferrous iron. Since the reaction rate depends on the concentration of reactant, the reaction rate of the first sub-step reaction is much higher than that of the second one (in #1 reactor). According to the theory of reaction rate controlling step (Nazemi et al., 2011), the overall reaction rate is determined by the lowest rate of the sub-step reaction. Thus, the oxidation reaction is mainly affected by the second sub-step reaction and the oxidation reaction rate is approximately equal to the rate of the second sub-step reaction in #1 reactor. While in #2 to #4 reactors, the concentration of ferrous iron is nearly 4 times that of oxygen and there are little difference between the reaction rate of Eqs. (5-a) and (5-b). Thus, the oxidation reaction is controlled by both Reactions (5-a) and (5-b). Finally, the oxidation rate r_1^i in #i reactor can be described as follows

$$r_1^i = \begin{cases} k_1^i(1+\eta^i C^i_{Cu^{2+}})(C^i_{O_2})^{\beta}(c_3^i)^{\gamma} & i=1 \\ k_1^i(1+\eta^i C^i_{Cu^{2+}})(x_1^i)^{\alpha}(C^i_{O_2})^{\beta}(c_3^i)^{\gamma} & i=2,\ 3,\ 4, \end{cases} \quad (6)$$

Table 2
The oxygen and ferrous iron concentration in four reactors (unit: mmol/L).

Parameter	#1 reactor	#2 reactor	#3 reactor	#4 reactor
$C_{Fe^{2+}}$	107.4–214.9	53.7–107.4	17.9–71.6	3.6–35.8
C_{O_2}	3.8–6.4	13.9–15.0	9.6–10.4	8.0–8.7

where k_1^i and η^i are the oxidation rate constant and the catalytic action coefficient in the #i reactor, respectively; $C_{Cu^{2+}}$ and C_{O_2} are the concentration of Cu^{2+} and O_2 in the #i reactor, respectively; $C^i_{O_2} = \ln(\lambda u_1^i + 1)$ (λ is the coefficient of dissolved oxygen); α, β, and γ are the reaction orders (based on experimental analysis (Verbaan and Crundwell, 1986), $\lambda = 0.1242$, $\alpha = 2$, $\beta = 1$, and $\gamma = -0.36$).

Secondly, as shown in Eq. (2), the ferric iron is hydrolyzed to goethite in the hydrolysis reaction, and the hydrolysis reaction rate r_2^i in #i reactor can be calculated by

$$r_2^i = k_2^i c_2^i, \qquad i = 1,\ 2,\ 3,\ 4, \quad (7)$$

where k_2^i denotes the hydrolysis rate constant in the #i reactor.

Thirdly, during the goethite process, the zinc oxide is used to neutralize the excess hydrogen ions, which is described in Eq. (3). The neutralization reaction rate r_3^i in #i reactor can be calculated by

$$r_3^i = k_3^i u_2^i c_3^i, \qquad i = 1,\ 2,\ 3,\ 4, \quad (8)$$

where k_3^i denotes the neutralization rate constant in the #i reactor.

Finally, since the inlet flow in #1 reactor consists of two parts (the leaching solution and the underflow), the dynamic model of #1 reactor (Fig. 2) is different from that in #2 to #4 reactors (Fig. 3). Considering the impure ion concentration of underflow is much lower than that of leaching solution (e.g., according to the data from real-life plant, the concentration of ferrous iron in the underflow is nearly 1/50 of that in the leaching solution, and the flow rate of underflow is about one third of that of the leaching solution), the influence of the concentration of underflow in #1 reactor can be ignored.

Based on the principle of material balance, the rates of the concentration change of the ferrous iron, the ferric iron, and the hydrogen ion in #i reactor can be described as

$$\dot{\mathbf{c}}^i = A_1^i \mathbf{c}_0^i + A_2^i \mathbf{c}^i + \boldsymbol{\phi}^i(\mathbf{c}^i, \mathbf{u}^i) = \mathbf{p}^i(\mathbf{c}^i, \mathbf{u}^i, t), \quad (9)$$

where

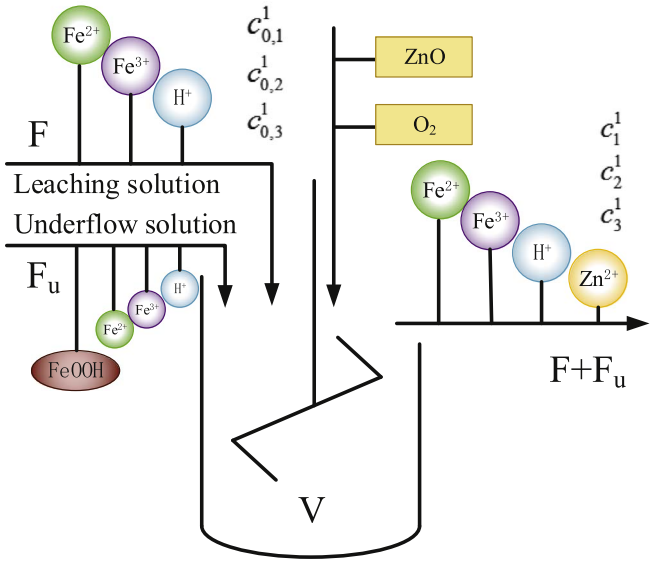

Fig. 2. The CSTR system for #1 reactor.

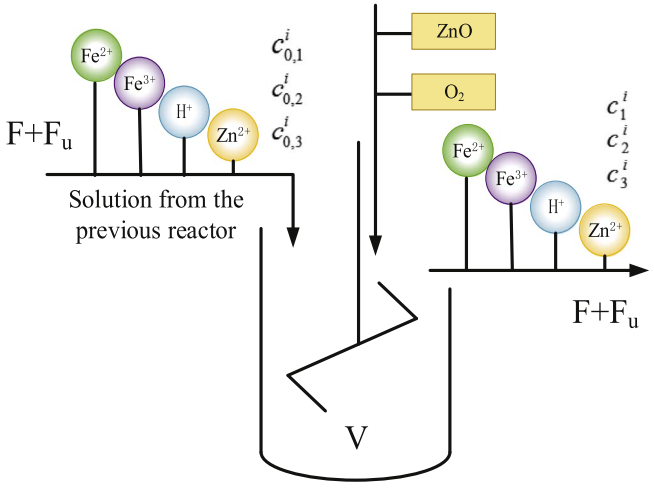

Fig. 3. The CSTR system for #2,#3,#4 reactors.

$$A_1^1 = \begin{bmatrix} \frac{F}{V} & 0 & 0 \\ 0 & \frac{F}{V} & 0 \\ 0 & 0 & \frac{F}{V} \end{bmatrix}$$

$$A_1^i = \begin{bmatrix} \frac{F+F_u}{V} & 0 & 0 \\ 0 & \frac{F+F_u}{V} & 0 \\ 0 & 0 & \frac{F+F_u}{V} \end{bmatrix} \quad i=2,\ 3,\ 4$$

$$A_2^i = \begin{bmatrix} -\frac{F+F_u}{V} & 0 & 0 \\ 0 & -\frac{F+F_u}{V} & 0 \\ 0 & 0 & -\frac{F+F_u}{V} \end{bmatrix} \quad i=1,\ 2,\ 3,\ 4$$

$$\boldsymbol{\phi}^i = \begin{bmatrix} -4r_1^i \\ 4r_1^i - r_2^i \\ -4r_1^i + 3r_2^i - 2r_3^i \end{bmatrix} \quad i=1,\ 2,\ 3,\ 4$$

2.2.4. The constraint of inlet ion concentration

Since the time of solution in the pipes between the reactors is relatively short when compared to the time of the solution reacting in the reactors and there are no additives in the pipes, the coupling effects occurring between two consecutive reactors can be ignored (Xie et al., 2015b) . Then the inlet reactant concentration of the #*i* reactor is the outlet reactant concentration of the #*i*-1 reactor ($i = 2,3,4$), which can be expressed as

$$\mathbf{c}_0^i = \mathbf{c}^{i-1}(t),\ i = 2,\ 3,\ 4. \tag{10}$$

2.2.5. The constraint of outlet ion concentration

On the basis of the technical requirement of the goethite process, the outlet concentration of ions must satisfy the specifications in Table 1, which can be described as

$$\begin{cases} c_{1,\min}^i \le c_1^i(t) \le c_{1,\max}^i,\ i=1,\ 2,\ 3,\ 4 \\ c_2^i(t) \le c_{2,\max}^i,\ i=1,\ 2,\ 3,\ 4 \\ c_{3,\min}^i \le c_3^i(t) \le c_{3,\max}^i,\ i=1,\ 2,\ 3,\ 4, \end{cases} \tag{11}$$

where $\mathbf{c}_{1,\min}^i$ and $\mathbf{c}_{3,\min}^i$ is the minimum concentration values of Fe^{2+} and H^+ in #*i* reactor, respectively; and $\mathbf{c}_{1,\max}^i$, $\mathbf{c}_{2,\max}^i$ and $\mathbf{c}_{3,\max}^i$ are the maximum concentration values of Fe^{2+}, Fe^{3+} and H^+ in #*i* reactor, respectively.

2.2.6. The constraint of the amounts of additive

According to equipment capacity and production requirements, the amounts of additive must be within the limits, which can be defined as

$$\begin{cases} u_{1,\min}^i \le u_1^i(t) \le u_{1,\max}^i,\ i=1,\ 2,\ 3,\ 4 \\ u_{2,\min}^i \le u_2^i(t) \le u_{2,\max}^i,\ i=1,\ 2,\ 3,\ 4, \end{cases} \tag{12}$$

where $u_{1,\min}^i$ and $u_{2,\min}^i$ are the allowed minimum amounts of oxygen and zinc oxide in #*i* reactor, respectively; $u_{1,\max}^i$ and $u_{2,\max}^i$ are the allowed maximum amounts, respectively.

2.2.7. The resulting dynamic multi-objective formulation and analysis

Based on the above analysis, the dynamic multi-objective optimization problem can be expressed as follows:

$$\begin{cases} \min & J_1 = \int_0^{T_f} (p_1 * u_1(t) + p_2 * u_2(t))dt \\ \max & J_2 = \dfrac{c_{0,1}^1(0) - c_1^4(T_f)}{c_{0,1}^1} \\ s.\ t. & \dot{\mathbf{c}}^i = \mathbf{p}^i(\mathbf{c}^i,\ \mathbf{u}^i,\ t) \\ & \mathbf{c}_0^i = \mathbf{c}^{i-1}(t),\ i=2,\ 3,\ 4 \\ & c_{1,\min}^i \le c_1^i(t) \le c_{1,\max}^i,\ i=1,\ 2,\ 3,\ 4 \\ & c_2^i(t) \le c_{2,\max}^i,\ i=1,\ 2,\ 3,\ 4 \\ & c_{3,\min}^i \le c_3^i(t) \le c_{3,\max}^i,\ i=1,\ 2,\ 3,\ 4 \\ & u_{1,\min}^i \le u_1^i(t) \le u_{1,\max}^i,\ i=1,\ 2,\ 3,\ 4 \\ & u_{2,\min}^i \le u_2^i(t) \le u_{2,\max}^i,\ i=1,\ 2,\ 3,\ 4. \end{cases} \tag{13}$$

The optimization problem of the iron precipitation process is a problem with high nonlinearity and strong coupling, and it is usually difficult to solve this type of problem (as shown in Fig. 4). On the one hand, since the state variables and control variables are the function of time rather than a scalar quantity, this kind of problem is an infinite dimensional problem (a common method is to convert the dynamic optimization problem into a finite-dimensional nonlinear programming problem based on variable discretization (Angira and Santosh, 2007; Kim et al., 2008)). Considering the discretization of both state variables and control variables will cause huge computational cost, the discretization method in this paper is only based on the control variables (the control interval is also optimally adjusted).

On the other hand, due to the presence of two production objectives

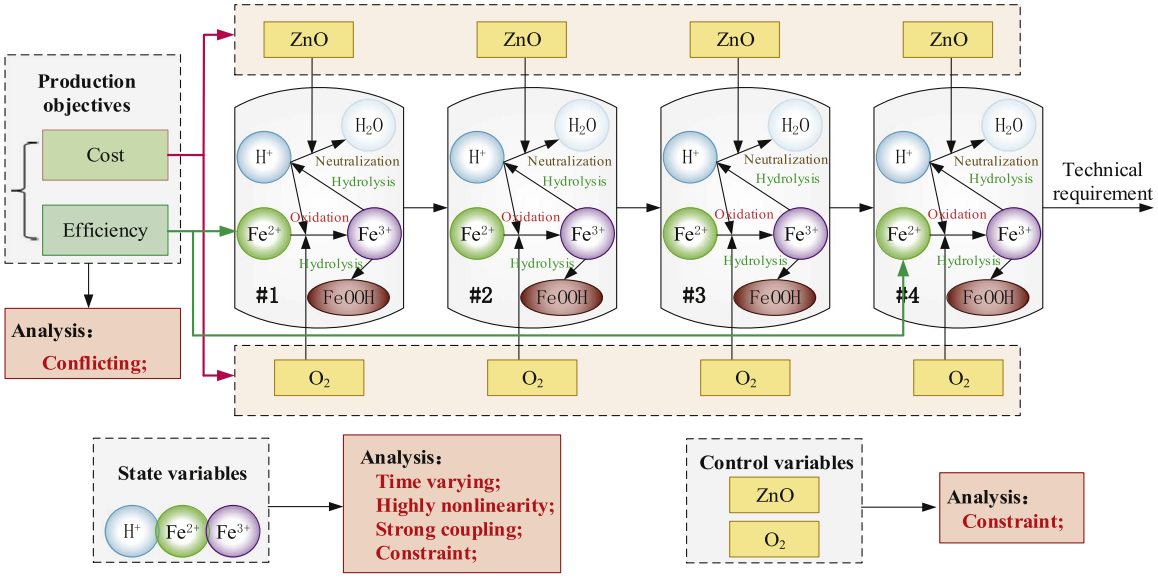

Fig. 4. The analysis for the optimization problem arising in the goethite process.

and many state constraints, it is necessary to use an appropriate optimization method to find its true Pareto solutions. The state transition algorithm (STA) (Zhou et al., 2013, 2012, 2014) is a stochastic optimization approach with strong global search ability. In this paper, a multi-objective optimization algorithm based on the STA and constrained nondominated sorting is proposed.

2.3. Discretization method based on control variable and control interval

The discretization method based on control variables is widely used in dynamic optimization problems. It divides the time span into several intervals, and uses basis functions with unspecified parameters to approximate the control variables (Shi, 2002). The common discretization method always sets the control intervals to equal length (Chen et al., 2014a), which cannot adjust the control period according to the characteristics of the practical problem. Take a bang-bang control problem for example, the optimal control trajectory is given as follows

$$\iota_{optimal}(t) = \begin{cases} 1, & if \quad t\in[0,\ 0.7] \\ 0, & if \quad t\in[0.7,\ 5]. \end{cases} \tag{14}$$

If the control intervals are set equally and the time span [0,5] is partitioned into 10 parts [0,0.5,1,…,4.5,5], the control trajectory can be obtained as

$$\iota_1(t) = \begin{cases} 1, & if \quad t\in[0,\ 0.5] \\ 0, & if \quad t\in[0.5,\ 5]. \end{cases} \tag{15}$$

The error between $\iota_{optimal}$ and ι_1 is $err_1 = \int_0^5 |\iota_1 - u_{optimal}|dt = 0.2$. In order to reduce the error, the time span is partitioned into 20 parts [0,0.25,0.5,…,4.75,5] and the control trajectory can be obtained as

$$\iota_2(t) = \begin{cases} 1, & if \quad t\in[0,\ 0.75] \\ 0, & if \quad t\in[0.75,\ 5]. \end{cases} \tag{16}$$

The error between $\iota_{optimal}$ and ι_2 is $err_2 = \int_0^5 |\iota_2 - \iota_{optimal}|dt = 0.05$. If the control intervals can be adjusted, the time span only need to be partitioned into 2 parts to obtain the optimal trajectory. Therefore, the non-uniform discretization method is more flexible. In addition, to improve the control precision, the number of control intervals in uniform discretization method is always set to a large value, which may increase the difficulty of the optimization problem and the complexity of the industrial operation (Chen et al., 2014b). Thus, in this paper, the time span is partitioned into multiple non-uniform intervals which is determined by optimization algorithm. For convenience, the control intervals are set the same for the two control variables (u_1^i and u_2^i). Thus, the time span $[0,T_f]$ of the optimization model are partitioned into N parts $[t_{n-1}^i, t_n^i](n = 1, 2, ...,N)$, which can be defined as follows

$$0 = t_0^i < t_1^i < t_2^i < ... < t_N^i = T_f. \tag{17}$$

In the goethite process, the control variables are approximated by piecewise constant function at optimized switching time. The vector of control parameters in each reactor is defined as

$$\boldsymbol{\kappa}^i = [\boldsymbol{\kappa}_1^i \ \ \boldsymbol{\kappa}_2^i \ \ ... \ \ \boldsymbol{\kappa}_N^i] = \begin{bmatrix} \kappa_{1,1}^i & \kappa_{1,2}^i & ... & \kappa_{1,N}^i \\ \kappa_{2,1}^i & \kappa_{2,2}^i & ... & \kappa_{2,N}^i \end{bmatrix}. \tag{18}$$

During the entire time span, the control variable can be described as

$$\mathbf{u}_n^i(t|\boldsymbol{\kappa}^i) = \sum_{n=1}^{N} \boldsymbol{\kappa}_n^i \theta_{[t_{n-1}^i, t_n^i)}^i(t), \tag{19}$$

where

$$\theta_{[t_{n-1}^i, t_n^i)}^i(t) = \begin{cases} 1, & t\in[t_{n-1}^i,\ t_n^i) \\ 0, & elsewhere \end{cases}$$

According to the Eq. (13), the dynamic optimization problem can be transformed to

$$\begin{cases} \min & J_1=\sum_{i=0}^{4}\sum_{n=0}^{N}\int_{t_{n-1}^i}^{t_n^i}(p_1*\kappa_{1,n}^i\theta_{[t_{n-1}^i,t_n^i)}^i(t)+p_2*\kappa_{2,n}^i\theta_{[t_{n-1}^i,t_n^i)}^i(t))dt \\ \max & J_2=\dfrac{c_{0,1}^1(0)-c_1^4(t_N^4)}{c_{0,1}^1} \\ s.\ t. & \dot{\mathbf{c}}^i(t)=\sum_{n=0}^{N}\mathbf{g}^i(\mathbf{c}^i(t),\boldsymbol{\kappa}^i)\theta_{[t_{n-1}^i,t_n^i)}^i(t),\ t\in[0,\ t_N^i) \\ & \mathbf{c}_0^i=\mathbf{c}^{i-1}(t|\boldsymbol{\kappa}^{i-1}),\ i=2,\ 3,\ 4 \\ & c_{1,\min}^i-c_1^i(t|\boldsymbol{\kappa}^i)\le 0,\ i=1,\ 2,\ 3,\ 4 \\ & c_1^i(t|\boldsymbol{\kappa}^i)-c_{1,\max}^i\le 0,\ i=1,\ 2,\ 3,\ 4 \\ & c_2^i(t|\boldsymbol{\kappa}^i)-c_{2,\max}^i\le 0,\ i=1,\ 2,\ 3,\ 4 \\ & c_{3,\min}^i-c_3^i(t|\boldsymbol{\kappa}^i)\le 0,\ i=1,\ 2,\ 3,\ 4 \\ & c_3^i(t|\boldsymbol{\kappa}^i)-c_{3,\max}^i\le 0,\ i=1,\ 2,\ 3,\ 4 \\ & u_{1,\min}^i-u_1^i(t|\boldsymbol{\kappa}^i)\le 0,\ i=1,\ 2,\ 3,\ 4 \\ & u_1^i(t|\boldsymbol{\kappa}^i)-u_{1,\max}^i\le 0,\ i=1,\ 2,\ 3,\ 4 \\ & u_{2,\min}^i-u_2^i(t|\boldsymbol{\kappa}^i)\le 0,\ i=1,\ 2,\ 3,\ 4 \\ & u_2^i(t|\boldsymbol{\kappa}^i)-u_{2,\max}^i\le 0,\ i=1,\ 2,\ 3,\ 4. \end{cases} \tag{20}$$

In Eq. (20), the vector of control parameters $\boldsymbol{\kappa}^i$ and the control intervals $[t_{n-1}^i,\ t_n^i](n=1,\ 2,\ ...,N)$ need to be determined. The decision variable $\mathbf{D}$ of optimization problem is defined as follows.

$$\begin{aligned}\mathbf{D} &= [\boldsymbol{\kappa}^i\ \ \mathbf{t}^i]=[\boldsymbol{\kappa}_1^i\ \ \boldsymbol{\kappa}_2^i\ \ ...\ \ \boldsymbol{\kappa}_N^i\ \ \mathbf{t}_1^i\ \ \mathbf{t}_2^i\ \ ...\ \ \mathbf{t}_{N-1}^i] \\ &= \begin{bmatrix} \kappa_{1,1}^i & \kappa_{1,2}^i & ... & \kappa_{1,N}^i & t_1^i & t_2^i & ... & t_{N-1}^i \\ \kappa_{2,1}^i & \kappa_{2,2}^i & ... & \kappa_{2,N}^i & t_1^i & t_2^i & ... & t_{N-1}^i \end{bmatrix}.\end{aligned} \tag{21}$$

2.4. Multi-objective optimization method based on the STA and constrained nondominated sorting

According to the optimization model of Eq. (20), the optimization problem not only has two objectives but also consists of many constraints. In this paper, a selection strategy based on constrained nondominated sorting is cooperated with the STA to deal with this kind of multi-objective optimization problem. Firstly, the STA is used to generate candidate solutions and then the selection strategy is adopted to choose the optimal solutions.

2.4.1. A brief description of the state transition algorithm

Based on the concepts of state transition and state space in control theory, the STA (Han et al., 2017b; Zhou et al., 2013, 2017, 2012, 2014) is proposed to deal with nonlinear nonconvex optimization problems. In the STA, every solution of the problem is regarded as a state, and the updating of current solution is considered as a state transition. The generating of the candidate solutions in the STA can be described as follows

$$\begin{cases} \mathbf{x}_{l+1}=A_l\mathbf{x}_l+B_l\boldsymbol{\nu}_l \\ y_{l+1}=f(\mathbf{x}_{l+1}), \end{cases} \tag{22}$$

where, $\mathbf{x}_l\in\mathbb{R}^n$ represents a candidate solution; A_l and B_l stand for transformation operators; $\boldsymbol{\nu}_l$ is a function of $\mathbf{x}_l$ and historical state; f is the objective function.

There are four special state transformation operators to generate candidate solutions.

(1) Rotation transformation

$$\mathbf{x}_{l+1}=\mathbf{x}_l+\varepsilon_a\frac{1}{w\|\mathbf{x}_l\|_2}R_r\mathbf{x}_l, \tag{23}$$

where ε_a is the rotation factor; $R_r\in\mathbb{R}^{w\times w}$, is a random matrix with its elements belonging to the range of $[-1,1]$ and $\|\cdot\|_2$ is the 2-norm of a vector. The rotation transformation can generate the candidate solution in a domain of a hypersphere with a given radius α, which is a local search operator.

(2) Translation transformation

$$\mathbf{x}_{l+1}=\mathbf{x}_l+\varepsilon_b R_t\frac{\mathbf{x}_l-\mathbf{x}_{l-1}}{\|\mathbf{x}_l-\mathbf{x}_{l-1}\|_2}, \tag{24}$$

where ε_b is the translation factor; $R_t\in\mathbb{R}$ is a random variable with its elements belonging to the range of [0,1]. The translation transformation has the function of line search which is only performed when a better solution can be found by other transformation operators.

(3) Expansion transformation

$$\mathbf{x}_{l+1}=\mathbf{x}_l+\varepsilon_c R_e\mathbf{x}_l, \tag{25}$$

where ε_c is the expansion factor; $R_e\in\mathbb{R}^{w\times w}$ is a random diagonal matrix with its elements obeying the Gaussian distribution with mean value 0 and standard deviation 1. The expansion transformation can search in the whole space, which is a global search operator.

(4) Axesion transformation

$$\mathbf{x}_{l+1}=\mathbf{x}_l+\varepsilon_a R_a\mathbf{x}_l, \tag{26}$$

where ε_d is the axesion factor; $R_a\in\mathbb{R}^{w\times w}$ is a random diagonal matrix with its elements obeying the Gaussian distribution with mean value 0 and standard deviation 1 and only one random position having nonzero value. The axesion transformation is designed for single dimensional search as well as global search.

For a given solution, the aforementioned state transition operators can generate many different candidate solutions. In this paper, the number of candidates generated by a certain operator is set to 40 and the transformation operators are alternately and independently applied in an iteration. To achieve a better understanding of the detailed steps of the STA, (Zhou et al., 2016) has proposed the Matlab toolbox for continuous state transition algorithm with single objective function.

2.4.2. Constrained nondominated sorting

From Eq. (20), the problem in the goethite process is a constrained multi-objective optimization problem, and all of the constraints are inequality constraints. For ease of understanding, several definitions are given as follows.

Definition 1 (*Feasible region*). The set of solutions that satisfy all constraints $g_{i_g}(\mathbf{x})\le 0$ $(i_g=1,2,...,m_g$, where m_g is the number of inequality constraints), is called the feasible region, which is described as: $\mathbb{F}=\{\mathbf{x}\in\mathbb{R}^n|g(\mathbf{x})\le 0\}$.

Definition 2 (*Constraint violation*). For the inequality constraints $g_{i_g}(\mathbf{x})\le 0$, $G_{i_g}(\mathbf{x})=\max\{0,\ g_{i_g}(\mathbf{x})\}^\nu$ is the violation of solution $\mathbf{x}$ on constraint g_{i_g}, where ν is normally 1 or 2. $G(\mathbf{x})=\sum_{i_g=1}^{m_g}G_{i_g}(\mathbf{x})$ is called the constraint violation of solution $\mathbf{x}$ on all constraints.

Definition 3 (*Pareto dominate*). For two objectives f_1 and f_2 in a minimization problem, the solution x_1' pareto dominates' (is better than) the solution x_2 is true when the following two conditions hold:

(1) $f_{i_f}(x_1)\le f_{i_f}(x_2)$, $i_f=1,\ 2$, which means that all objective values of x_1 are not worse than x_2;

(2) $\exists\ i_f=1,\ 2,\ s.\ t.\quad f_{i_f}(x_1)<f_{i_f}(x_2)$, which means that at least one objective value of x_1 is better than that of x_2.Because of the presence of constraints, the definition of *domination* between two solutions in a minimization problem is modified as follows.

Definition 4 (*Constrained dominate*). A solution x_1 constrained-dominates a solution x_2, if any of the following conditions is true.

(1) Solution x_1 is feasible and solution x_2 is infeasible.

(2) Both solutions are infeasible, but solution x_1 has smaller constraint violation.
(3) Both solutions are feasible, but solution x_1 pareto dominates solution x_2.

Definition 5 (*Pareto-optimal solution*). In the decision space, a set of optimal solutions is called the Pareto-optimal solution (POS) if none of the other solutions dominates any of them.

Definition 6 (*Pareto-optimal front*). The mapping of POS in the objective space is called the Pareto-optimal solution (POF).

When selecting optimal solutions from the candidate solutions, there are two strategies in this part.

Firstly, in order to reduce the computational complexity, for each solution x_τ, the number of solutions m_τ which constrained dominate x_τ is calculated, and the set of solutions S_τ that x_τ constrained dominate is obtained. If $m_\tau = 0$, the solution x_τ belongs to the first nondominated front. Then, for each solution x_τ with $m_\tau = 0$, we visit each member x_ς of the set S_τ and reduce its constrained domination count by one. If for any member x_ς the constrained domination count becomes zero, these members belong to the second nondominated front. The process continues until all fronts are identified (Deb et al., 2002; Peng et al., 2013; Wang et al., 2011).

Secondly, in order to preserve the diversity of optimal solutions, we investigate the strategy of crowding distance (Deb et al., 2002). For two objective functions f_1 and f_2, the crowding distance $P[i_s]_{distance}$ of solution x_{i_s} in a nondominated set P is defined as follows:

$$P[i_s]_{distance} = \frac{f_1(x_{i_s+1}) - f_1(x_{i_s-1})}{f_1^{\max} - f_1^{\min}} + \frac{f_2(x_{i_s+1}) - f_2(x_{i_s-1})}{f_2^{\max} - f_2^{\min}}, \quad (27)$$

where i_s is the solution number in a nondominated set. $f_1^{\max}$, $f_1^{\min}$ and $f_2^{\max}$, $f_2^{\min}$ are the maximum and minimum values of f_1 and f_2, respectively. Based on the nondominated front and the crowding distance, if two solutions belong to different fronts, the solution with lower (better) rank is preferred, and if both solutions belong to the same front, the solution with larger crowding distance is preferred.

The flow chart of the STA for solving multi-objective optimization problem in the goethite process is shown in Fig. 5.

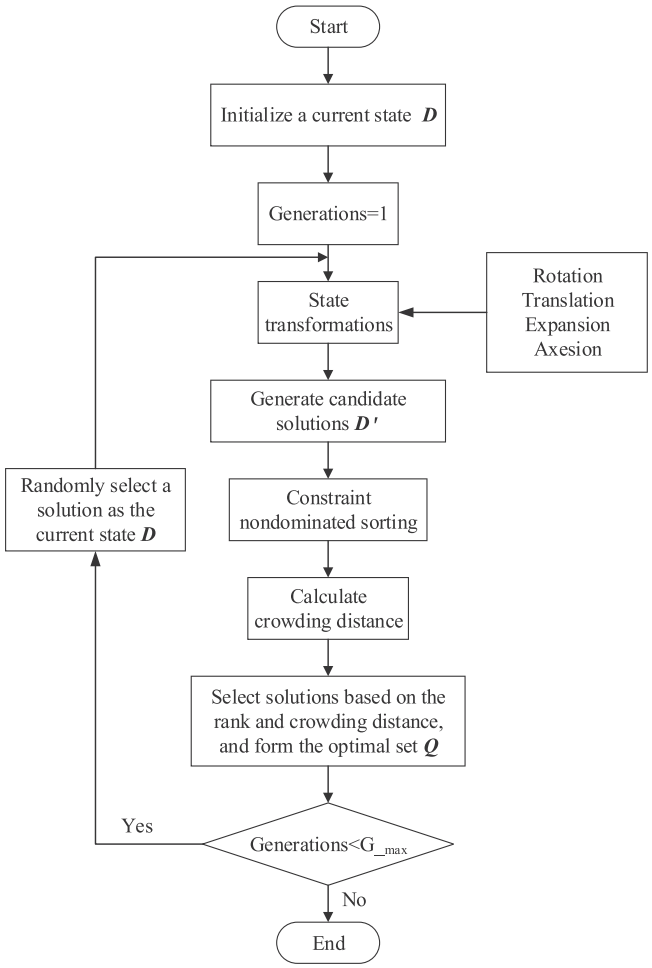

Fig. 5. The flow chart of multi-objective optimization algorithm based on the STA and constrained nondominated sorting.

2.5. Evaluation mechanism

After using the multi-objective optimization algorithm based on the STA to solve this problem, a set of optimal solutions of the amounts of additive is obtained. In order to choose the best one for industrial applications, an evaluation mechanism based on the concentration of ions and their trends is proposed. There are two parts in this mechanism: (1) the trends of the concentration of ions at each switching time in each reactor; (2) the outlet concentration of ions and their trends in each reactor.

In the first part of the evaluation mechanism, on the basis of the optimal set $\mathbf{Q} = \{Q_1, Q_2, \ldots, Q_m\}$, the differentials of the concentration of ions in #i reactor ($i = 1,2,3,4$) at switching time t_n ($n = 1,2,\ldots,N$) are computed, which represent the trends of the concentration. Fig. 6 illustrates the changing-curve of ion concentration. The solid line shows the performance of the slow control, where the change of ion concentration tends to be slow at each switching time. The dotted line indicates the performance of the fast control and there is a significant downward trend in ion concentration at each switching time. Although the dotted line can change the ion concentration in a short time, the fast control is inoperable in the goethite process: (i) take the ferrous iron for example, the fast control will make the ferrous iron oxidize too much in a short time and it is easily to form ferric hydroxide; (ii) since there is a sharp tendency at each switching time in the fast control, once the switching time is deviated, the ion concentration will be greatly changed and the control accuracy will be reduced. While in the slow control, even if the switching time exists deviation, the ion concentration will not have a great change and the whole control performance will not be influenced a lot; (iii) since the fast control has a strict requirement on the accuracy of switching time, it will result in high equipment costs to guarantee control effect. In addition, the ion concentration of slow control can reach the target value in the specified

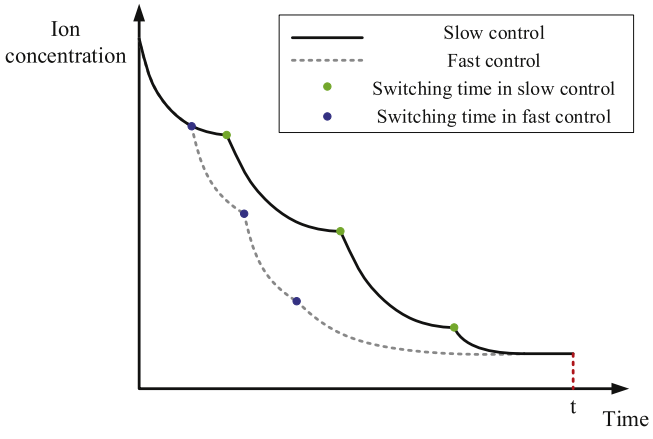

Fig. 6. The changing-curve of ion concentration.

time t, thus the slow control is more suitable for the goethite process. According to Eq. (9), the closer the differential is to zero, the more steady the ion concentration is (as well as the switching time). The evaluation function of this part is defined as follows.

$$E_1(Q_j) = \sum_{i=1}^{4}\sum_{n=1}^{N} |\dot{\mathbf{c}}^i(t_n, Q_j)|, \qquad j = 1, 2, \ldots, m. \tag{28}$$

In the second part of the evaluation mechanism, for each optimal solution, the outlet concentration of ions ($\mathbf{c}_j^i(t)$) and their differentials in #i reactor ($i = 1,2,3,4$) are computed. The ion concentration can reflect the feasibility of the solution and their trends can represent the future state of the ion concentration. A sharp trend can cause the ion concentration to return to the desired situation from an undesired situation, whereas it can also cause ion concentration to depart from the desired situation. When the ion concentration is within the acceptable range without fluctuation, the reaction process must be in a steady state. When the ion concentration is acceptable but has a sharp tendency that causes concentration changed, the process can not be considered qualified. In contrast, when the ion concentration exceeds the limits but with a good tendency for the concentration to return to the desired range, the situation is not as terrible as it seems to be. To address the uncertainty of the complex nature between the concentration and the process state, fuzzy logic is used to evaluate the performance of the optimal solution. In this paper, based on their upper and lower bounds, the concentration of ions are transformed into five linguistic variables namely VL (Very Low), LL (Little Low), S (Stable), LH (Little High), VH (Very High). The trends of concentration are also classified into five parts: NB (Negative Big), NS (Negative Small), Z (Zero), PS (Positive Small), PB (Positive Big). At the same time, the evaluation results are defined as seven grades, which is HN (High Negative), MN (Middle Negative), LN (Low Negative), Z (Zero), LP (Low Positive), MP (Middle Positive), HP (High Positive). Fig. 7 (a–c) show the membership function of all variables respectively. In Fig. 7 (a), b and d are the lower and upper bounds of the concentration respectively, and $c = (b + d)/2$, $a = (3b - d)/2$, $e = (3d - b)/2$. In Fig. 7 (b), $g = (d - b)/T_f$. Fig. 7 (d) shows the relationship between two inputs (concentration of ions and their trends) and one output (evaluation grade). The fuzzy rules for the inputs and output are given in Table 3. In this paper, the rules are established by previous analysis of the process.

Table 3
Fuzzy rules for the inputs and output.

Ion concentration	Differential of concentration				
	NB	NS	Z	PS	PB
VL	HN	HN	HN	MN	MN
LL	MN	MN	LN	LN	LN
S	LN	Z	Z	Z	LP
LH	LP	LP	LP	MP	MP
VH	MP	MP	HP	HP	HP

Since the output of the fuzzy system is a fuzzy value, the centroid defuzzification method is adopted to convert the evaluation grade to a real value $\mathbf{e}^*$. Thus, the evaluation function of this part for optimal set $\mathbf{Q} = \{Q_1, Q_2, \ldots, Q_m\}$ can be calculated by follows.

$$E_2(Q_j) = \sum_{i=1}^{4} |\mathbf{e}^{*,i}(Q_j)|, \qquad j = 1, 2, \ldots, m. \tag{29}$$

After computing those two parts of the evaluation functions, the best solution for industrial application can be determined by minimizing the overall evaluation functions, which is given by Eq. (30).

$$\min \quad E(Q_j) = E_1(Q_j) + E_2(Q_j), \qquad j = 1, 2, \ldots, m. \tag{30}$$

2.6. Strategy diagram of optimal process control

The strategy diagram of the optimal control in the iron precipitation process is shown in Fig. 8. Based on the mechanism model and technical requirements, the dynamic multi-objective optimization model is established. The discretization method based on control variable and control interval is used to convert the dynamic optimization problem into a nonlinear mathematical programming problem, and the STA cooperated with constrained nondominated sorting is proposed to solve the optimization problem. By using this optimization method, a set of optimal solutions is obtained. In order to select the best solution for industrial application, the evaluation mechanism is proposed which

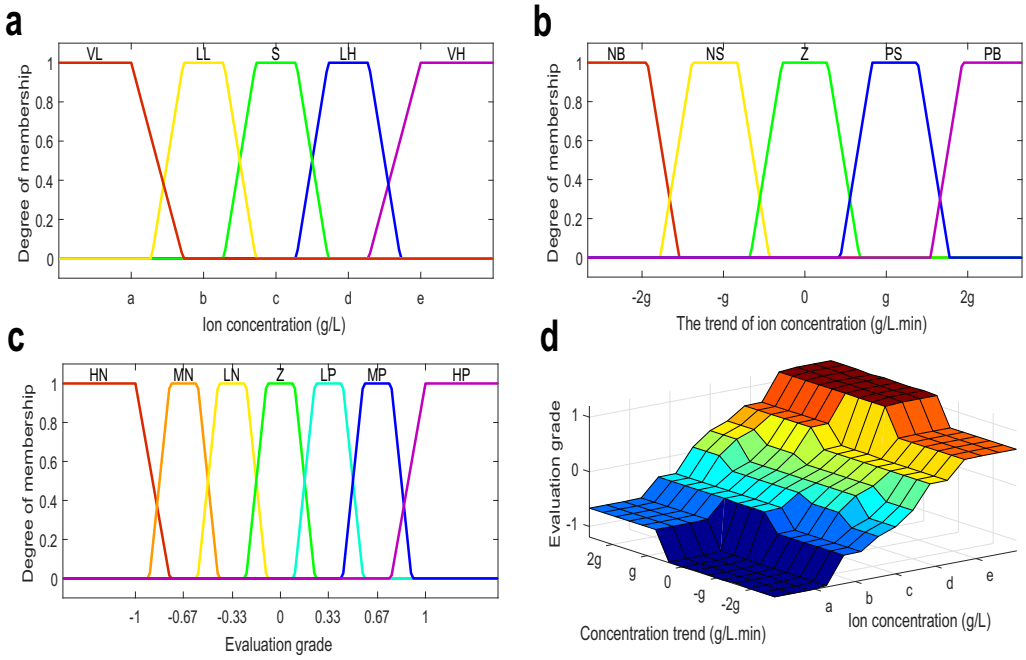

Fig. 7. Fuzzy logic evaluation system: (a) the memberships of ion concentration and the linguistic variables are VL (Very Low), LL (Little Low), S (Stable), LH (Little High), VH (Very High); (b) the memberships of the trend of ion concentration and the linguistic variables are NB (Negative Big), NS (Negative Small), Z (Zero), PS (Positive Small), PB (Positive Big); (c) the memberships of evaluation grade and the grades are HN (High Negative), MN (Middle Negative), LN (Low Negative), Z (Zero), LP (Low Positive), MP (Middle Positive), HP (High Positive); (d) the relationships among the evaluation grade, ion concentration and its trend.

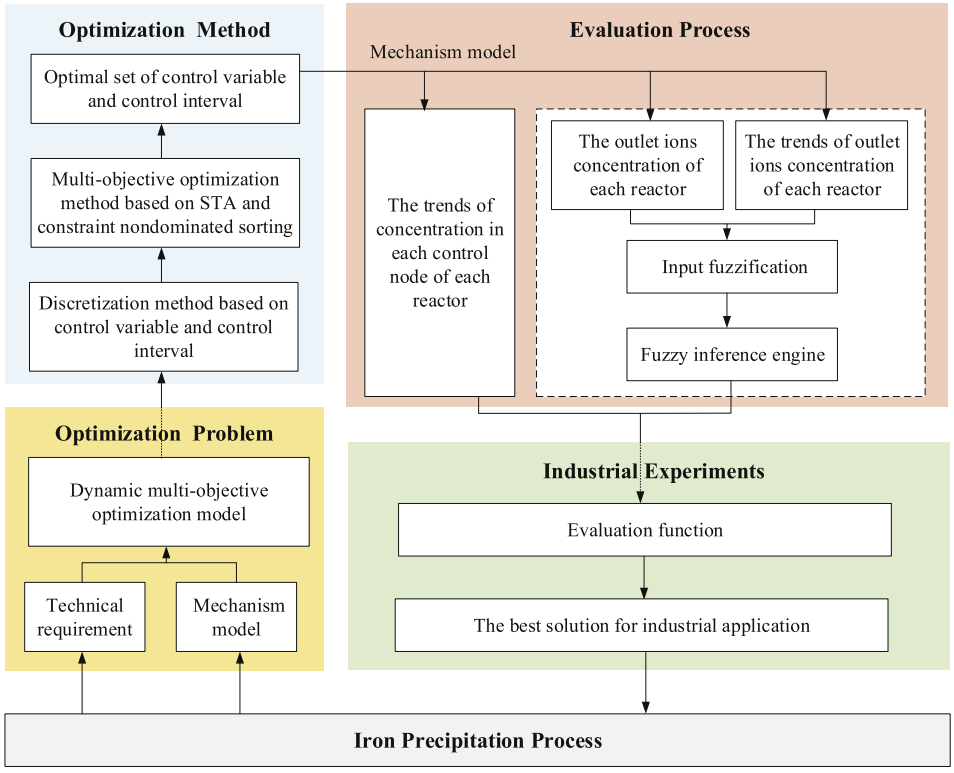

Fig. 8. The strategy diagram of the optimal control in the iron precipitation process.

consists of two parts: the first considers the concentration trends at each switching time in each reactor, the second considers the outlet concentration and their trends in each reactor. Moreover, in the second part, fuzzy logic is used to deal with the uncertainty of the complex nature. Finally, the effectiveness of the proposed methods and strategies is verified by industrial experiments.

3. Results and discussion

In this paper, we investigate the goethite process in a certain zinc hydrometallurgy plant in China, and the industrial data in May 2015 is collected for analysis. In the goethite process, the flow rate is measured on-line and the ion concentration is accessed every 2 h. Since the inlet ion concentration in the reactor fluctuates in a small range for a period of time under normal production condition, the measurement delay is ignored in our proposed method. The time of solution from the #1 reactor to #4 reactor is approximately 8 h, which means the terminal time in the optimization problem (T_f) is 480 min. The kinetic model of the goethite process has been validated by our research group (Xie et al., 2017), and in this study, we have performed some simulations to verify the effectiveness of the proposed method in the optimization of the goethite process. In manual control, 8-h shifts schedule is adopted in the zinc hydrometallurgy plant and the rate of oxygen and zinc oxide to be added in different reactors are adjusted according to the experience of the operators working in each shift. The simulations in this paper are carried out for 48 h(6 shifts), and the flow rate of leaching solution and underflow are shown in Fig. 9 (a). The inlet concentration of ferrous iron, ferric iron and the pH value are described in Fig. 9 (b).

In order to solve the dynamic multi-objective optimization problem in the goethite process, a discretization method based on control variable and control interval is explored and a multi-objective optimization method based on the STA and constrained nondominated sorting is proposed in this paper. All of the simulations are run under the MATLAB (Version R2016a) software platform. The parameter settings of the STA are shown as follows: α is reducing periodically from 1 to 1e−4 in an exponential way, β,γ and δ are all set to 1. All parameter settings are based on previous papers (Han et al., 2017a; Wang et al., 2016; Xie et al., 2016). To analyze the performance of the proposed multi-objective optimization method based on the STA (MOSTA), the comparisons between MOSTA and nondominated sorting genetic algorithm II (NSGAII) (Deb and Agrawal, 1995) are conducted. NSGAII is a computationally fast and elitist algorithm based on a nondominated sorting approach which is proposed by Deb and Agrawal (1995). After combining the existing parameter settings of NSGAII in previous papers, the crossover probability of $p_c = 0.9$ and a mutation probability of $p_m = 1/n$ (where n is the number of decision variables) are used (Deb and Agrawal, 1995).

In order to compare the computational cost of NSGAII and MOSTA, the average execution time of these two optimization algorithms is analyzed. For each shift, 10 independent runs are performed and the average execution time (seconds) of the optimization algorithms using 2.6 GHz Intel i5 PC with 8 G RAM is shown in Table 4. In terms of the information of Table 4, we can find that the speed of MOSTA is almost equal to that of NSGAII. For example, in the first sample, the execution time of MOSTA is 743.5317 s and the time of NSGAII is 767.1249 s.

Figs. 10 to 12 illustrate the cost and the efficiency, as conflicting objectives, in the 1st to 6th shifts. The color of each point shows the evaluation value of each optimal solution. Based on the evaluation mechanism in Section 2, the solution with the smallest evaluation value is chosen as the best one for industrial application. It is obvious that the Pareto-optimal front obtained by MOSTA can constrained dominate most solutions of NSGAII. That means the proposed multi-objective optimization algorithm in this paper has competitive results when compared with NSGAII (Deb et al., 2002). The evaluation value of

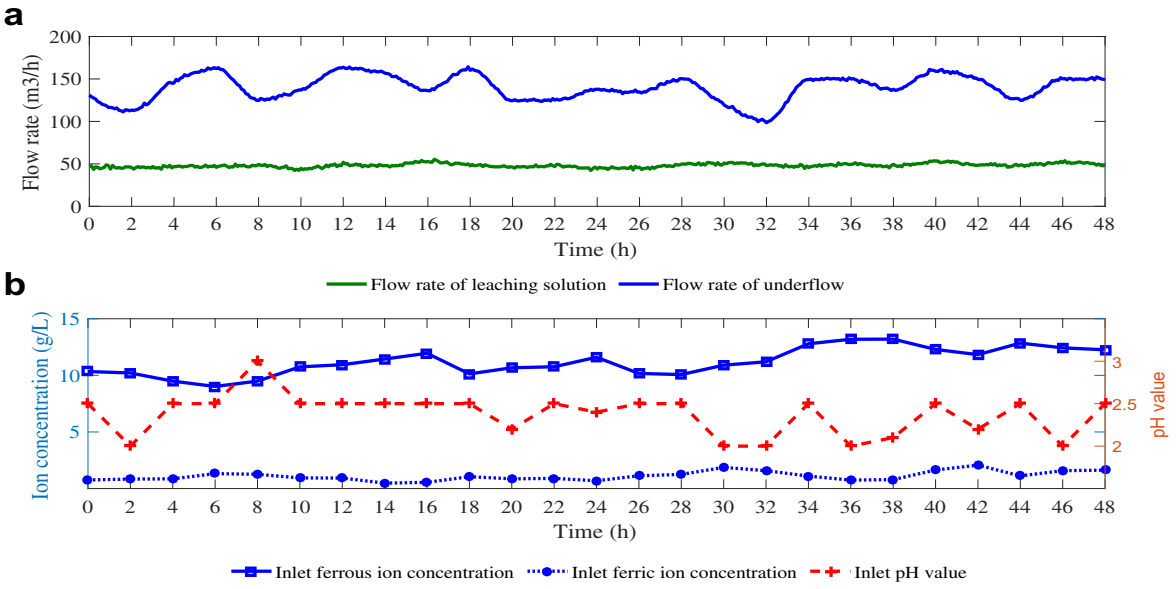

Fig. 9. Inlet flow rate and the concentration of ions of the goethite process.

Table 4
The average execution time (seconds) of all test.

Test	NSGAII	MOSTA
Shift 1	767.1249	743.5317
Shift 2	747.9778	738.0382
Shift 3	687.5559	673.5615
Shift 4	673.4471	668.6814
Shift 5	734.8874	722.1651
Shift 6	777.2505	764.5339

NSGAII is omitted in this paper since most of its optimal solutions are dominated by MOSTA. According to the data obtained from a real-life factory, in the 1st shift, the cost and the efficiency of manual control is 4.9959e5 ($/h) and 0.9464 (%) respectively, which are worse than the optimal control'. The same is true for other shifts.

The simulated outlet ferrous iron concentration, ferric iron concentration and pH value in each reactor are shown in Fig. 13. We can find that in #1 reactor, the ferrous iron concentration is always in the desired range of 6 g/L to 8 g/L, and the ferric iron concentration is also < 2 g/L in the whole time. The pH value in #1 reactor also belongs to the range of 2.7 to 3.5. Moreover, the concentration of ions in #2, #3 and #4 reactor all satisfy the requirements of the effluent, which means the best solution obeys the constraints in the optimization problem and indicates the feasibility of the best solution. Since the ferrous iron is the most interesting ion in the goethite process, and the ferric iron concentration is relative small and pH in the reactor is maintained at about 3.0, we mainly focus on the concentration of outlet ferrous irons in each reactor in this paper.

To verify the correctness of the evaluation mechanism, the simulated variations of the ferrous iron concentration in the 1st shift is shown in Fig. 14. According to the first part of evaluation mechanism, the smaller the ion concentration changes at the switching time, the more steady the process is. The second part of evaluation mechanism combines the information of outlet ion concentration and its trend.

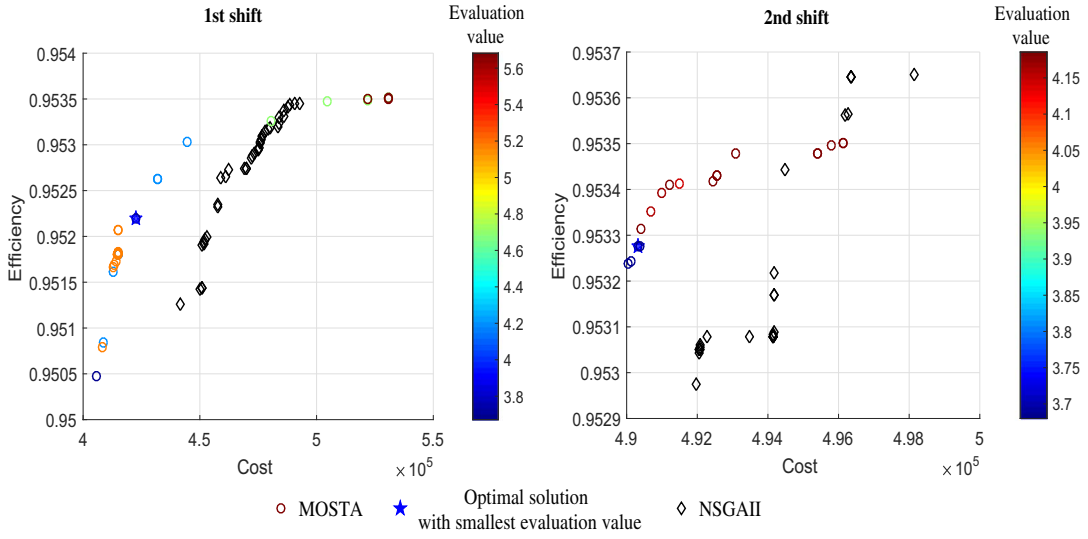

Fig. 10. Optimal solutions with evaluation mechanism in the 1st and 2nd samples.

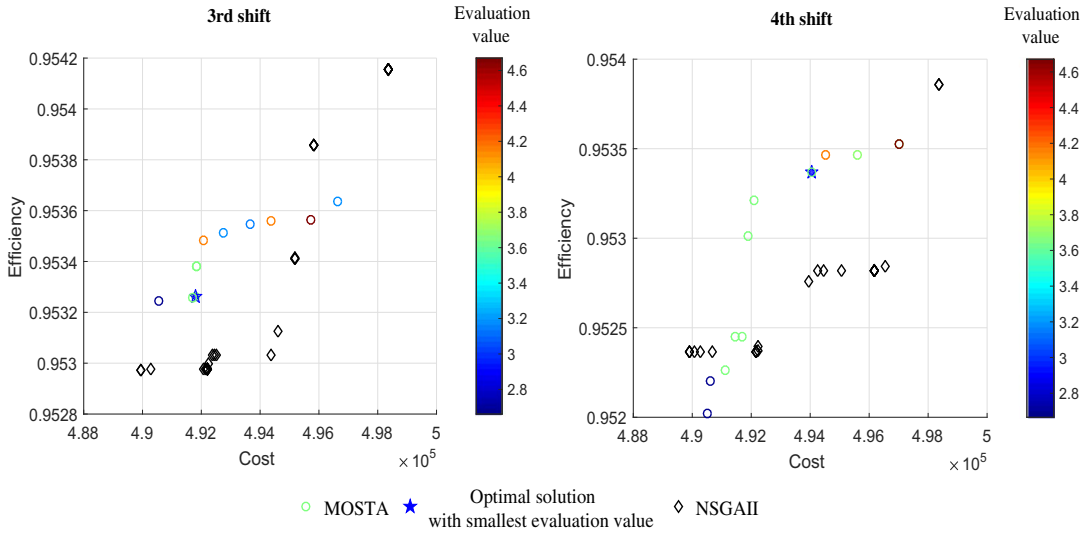

Fig. 11. Optimal solutions with evaluation mechanism in the 3rd and 4th samples.

Therefore, the desired condition is as follows: on the one hand, the iron concentration tends to be unchanged at each switching time; on the other hand, the iron concentration at other times is in the acceptable situation without too much fluctuation. In Fig. 14, the concentration of the blue line usually only changed when its trend is steady. Compared with the pink line and the green line, there are less fluctuations in the blue line, especially in the #4 reactor. Therefore, the result with the smallest evaluated value is more stable than the result with the larger evaluated value. That shows the effectiveness of the evaluation mechanism.

The optimization results show the feasibility of the optimization strategy and the evaluation mechanism. In order to show the superiority of the proposed method, the detailed comparisons between manual control and optimal control are shown below. Fig. 15 shows the comparisons of the cost and efficiency by manual control and optimal control. In practice, the operators always add excess oxygen and zinc oxide to ensure the quality of production, resulting in a lot of waste. Therefore, the costs under manual control are much larger than optimal control. At the same time, the efficiency of the ion precipitation process has been improved under the optimal control. The detailed additions of oxygen and zinc oxide set by two different control strategies are shown in Fig.s 16 and 17 respectively. Although the additions of manual control are sometimes less than the amounts of proposed control, the average cost of manual control is still more than optimal control's.

Fig. 18 shows the simulated outlet ferrous iron concentration from #4 reactor under manual control and optimal control respectively. The manual control of precipitation process depends largely on operator's experience, and if the operator is inexperienced or the operation is untimely, the outlet ferrous iron concentration may fluctuate significantly. Based on the control strategy proposed in this paper, the outlet ferrous iron concentration is closer to lower bounds of its targeted range with small fluctuations.

Table 5 is the performance of manual control and optimal control in the goethite process. Compared with manual control, the daily average additions of oxygen and zinc oxide under the proposed control decrease by 778.0854 m^3 /day and 4.9013 t/day, respectively. From the mean value and the fluctuation range of the outlet ferrous iron concentration in #4 reactor, it is observed that the outlet ferrous iron concentration in

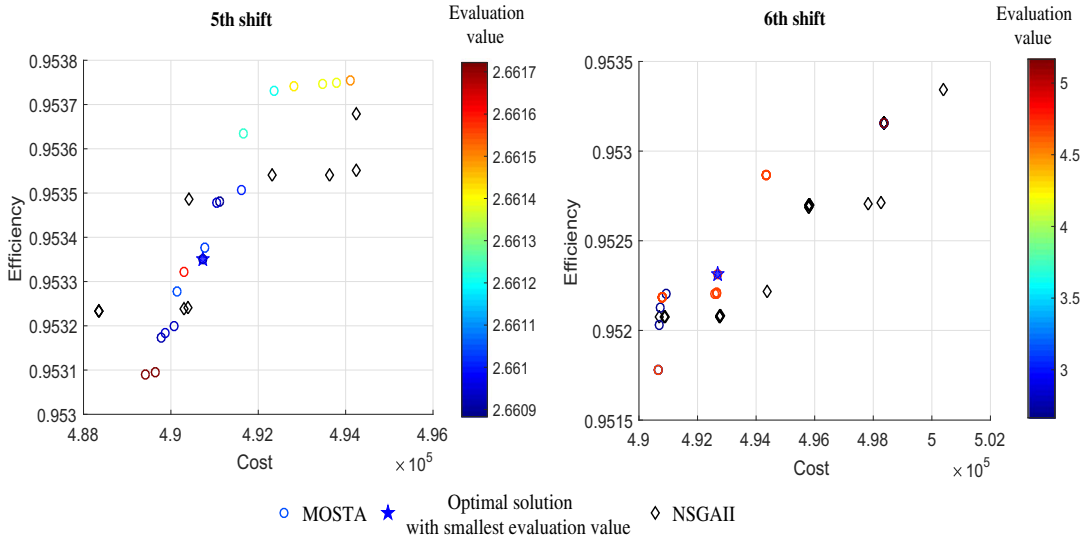

Fig. 12. Optimal solutions with evaluation mechanism in the 5th and 6th samples.

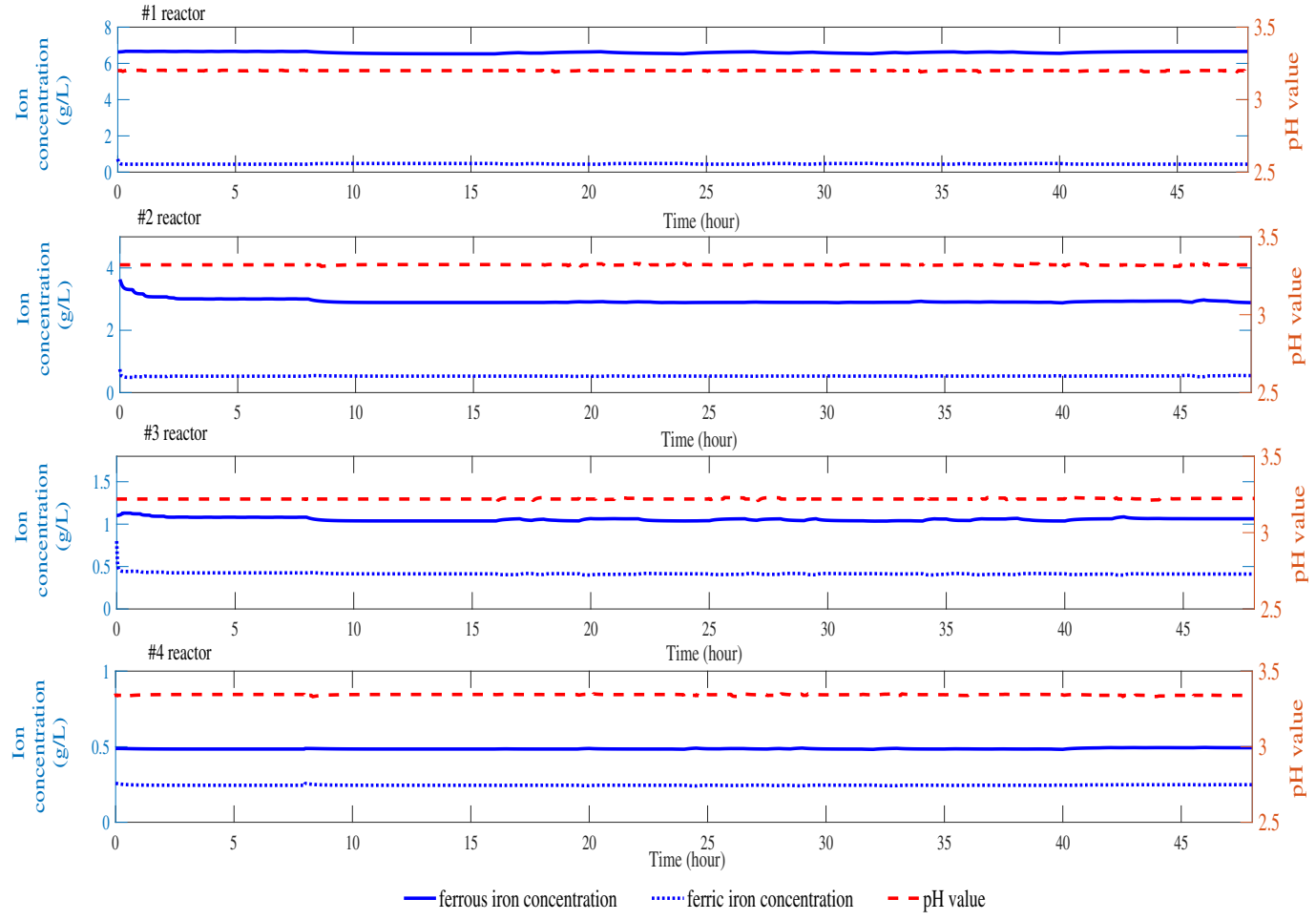

Fig. 13. The outlet ferrous iron concentration, ferric iron concentration and pH value in each reactor.

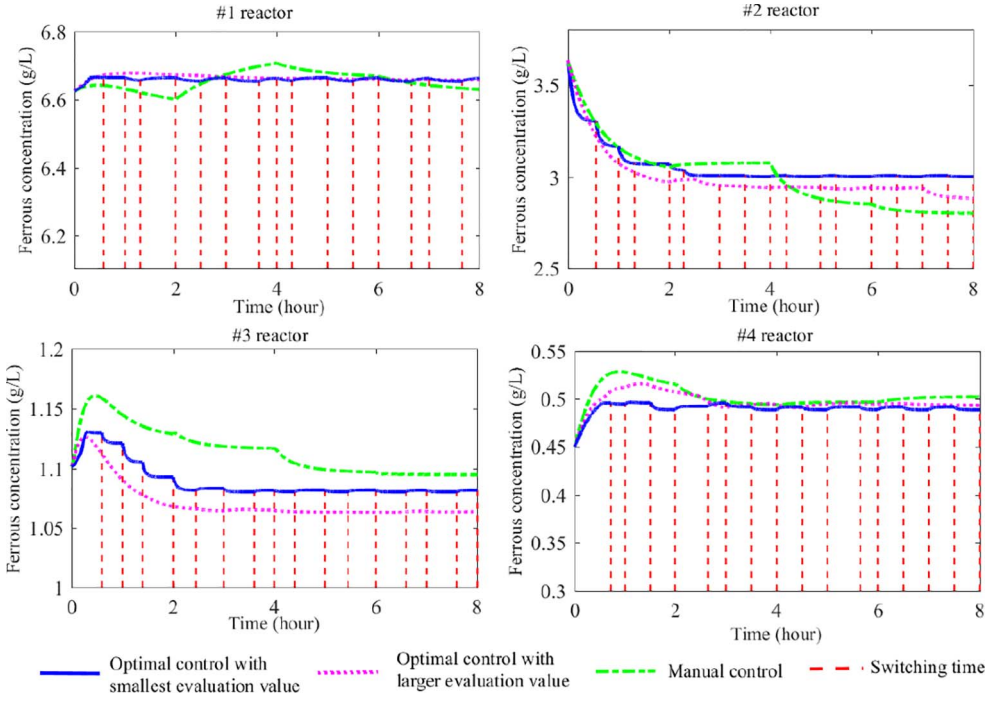

Fig. 14. The variations of the ferrous iron concentration in four reactors.

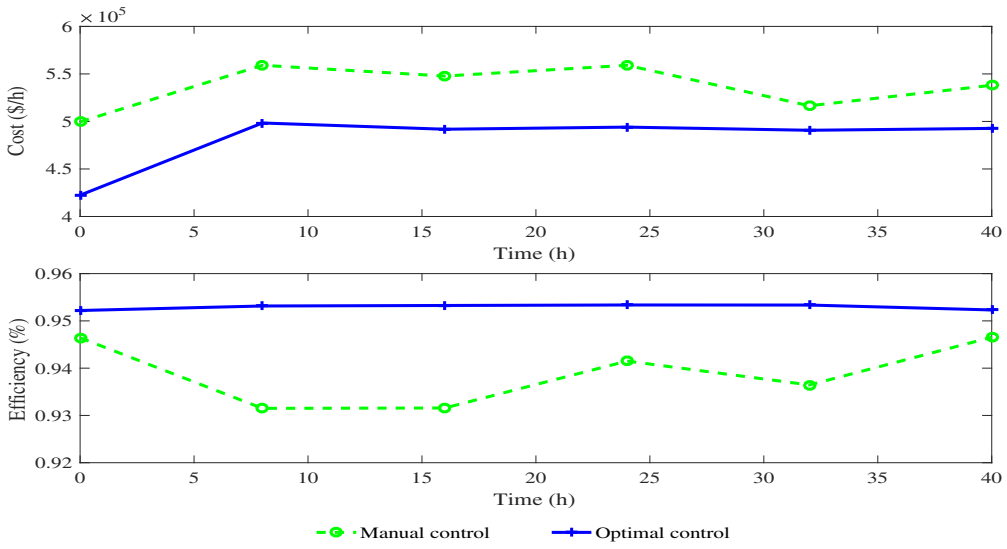

Fig. 15. Comparisons of the cost and efficiency by two control strategies.

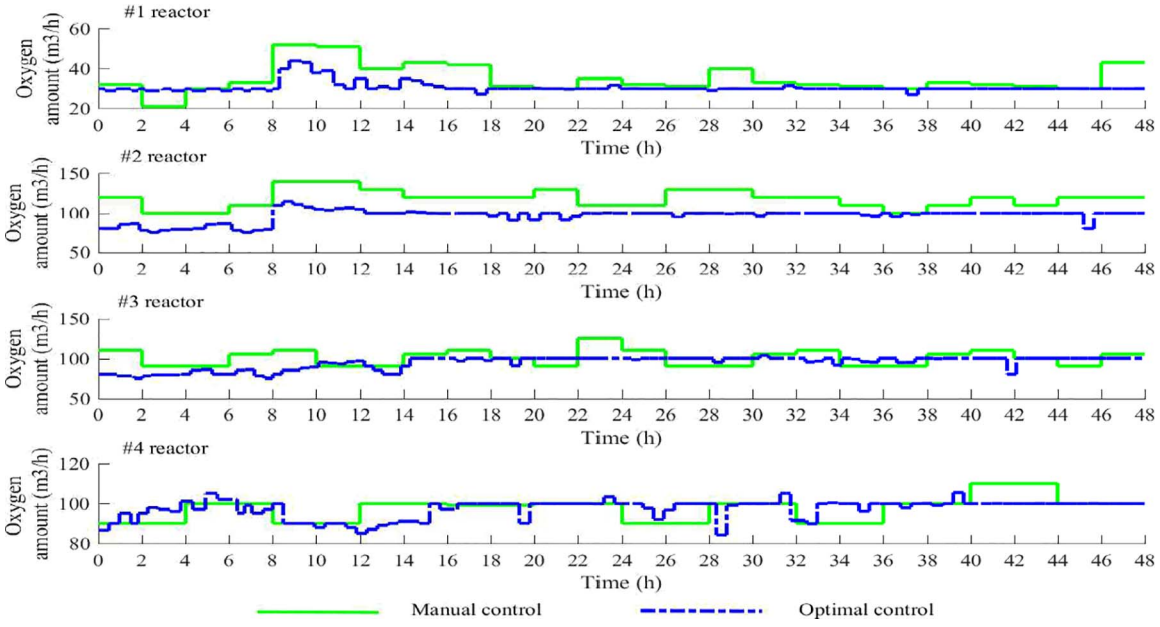

Fig. 16. Oxygen amounts setting by two different control strategies.

manual control usually fluctuate over a wide range. But by applying the optimal control strategy, the outlet ferrous iron concentration is much more stable. From simulation results, the proposed method could not only reduce the cost of the process as well as improve its efficiency, but also make the outlet concentration of ions more stable within the required ranges. Since the stability of outlet ion concentration in the goethite process plays an important role in subsequent process such as solution purification and electrowinning, the method proposed in this paper also has a positive effect on the whole process of zinc hydrometallurgy.

4. Conclusions

Based on the technical requirements and the chemical kinetics in the goethite process, a dynamic optimization model is established to minimize the cost of reagents and maximize the efficiency of iron precipitation simultaneously. A discretization method based on control variable and control interval is proposed to transform the dynamic problem to a nonlinear mathematical programming problem. Then, the constrained nondominated sorting is cooperated with the STA to solve multi-objective nonlinear programming. An evaluation mechanism is proposed to choose the best solution for industrial applications. In this mechanism, the information of the concentration and their trends are used for analysis. The simulation results have illustrated that the proposed multi-objective state transition algorithm has competitive performance compared with NSGAII. Furthermore, the optimal control has better control results than manual control in terms of the cost and the efficiency.

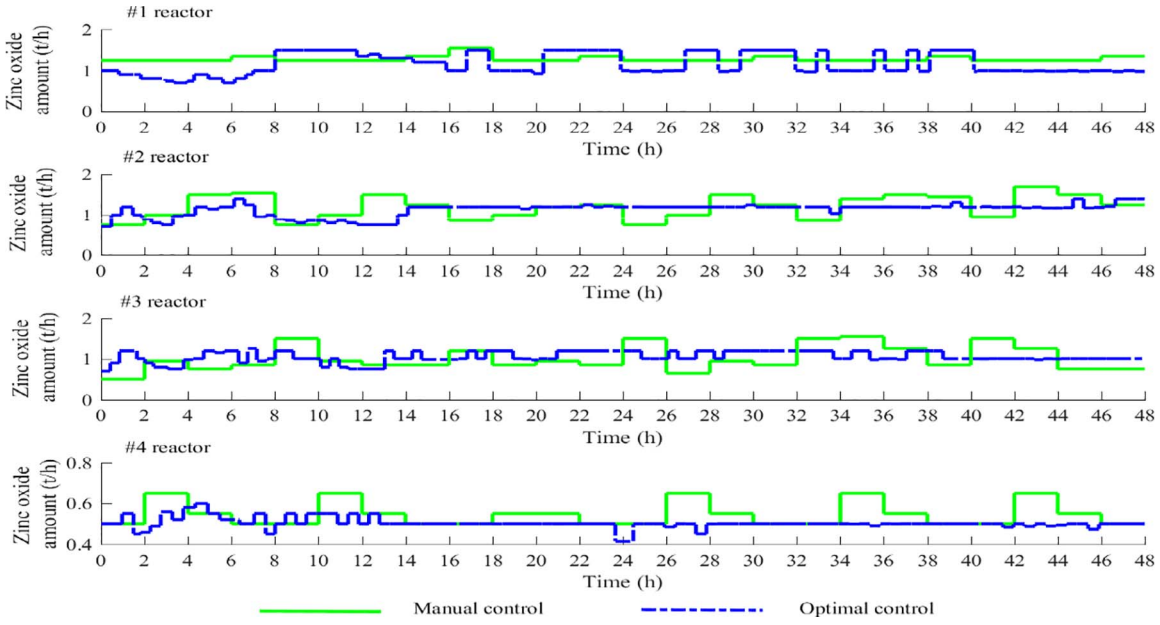

Fig. 17. Zinc oxide amounts setting by two different control strategies.

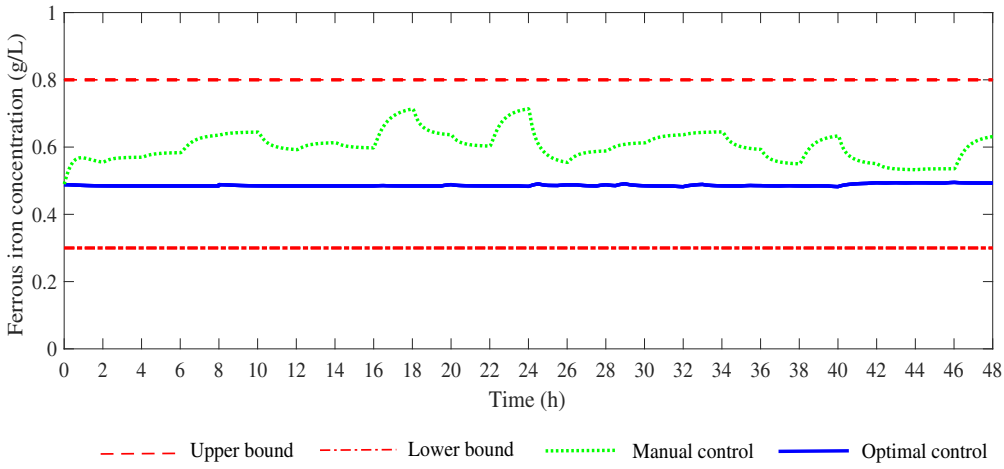

Fig. 18. Comparisons of the outlet ferrous iron concentration from #4 reactor by two control strategies.

Table 5
Comparison of the control performance by manual control and optimal control.

Methods	The outlet ferrous iron concentration			Average amount of additive		Efficiency
	Mean value (g/L)	Qualification rate (%)	Fluctuation range (g/L)	Oxygen (m^3/day)	Zinc oxide (t/day)	
Manual control	0.6032	100	[0.4900,0.7139]	8426.0001	97.1000	93.90%
Optimal control	0.4864	100	[0.4822,0.4950]	7647.9147	92.1987	95.29%

Notation

Equipment

BK	Zinc Oxide Bunker
R	Reactor
T	Overflow Tank
FP	Filter Press
TH	Thickener

Variable

α, β, γ	the reaction orders of oxidation reaction
λ	the coefficient of dissolved oxygen
η_i	the coefficient of catalytic action in $\#i$ reactor
ε_a	the rotation factor in the state transition algorithm
ε_b	the translation factor in the state transition algorithm
ε_c	the expansion factor in the state transition algorithm
ε_d	the axesion factor in the state transition algorithm
θ^i	the piecewise constant functions in $\#i$ reactor
κ^i	the vector of control parameters in $\#i$ reactor
A, B	the transformation operators in the state transition algorithm
D	the decision variables in optimization problem
E_1	the first part evaluation value
E_1	the second part evaluation value
E	the total evaluation value
F	the flow rate of the leaching solution
F_u	the flow rate of the underflow
G	the overall constraint violation
G_{i_g}	the i_gth constraint violation
I_{max}	the max iteration number in optimization algorithm

J_1, J_2	the objective functions in the iron precipitation process
$P[i_s]_{distance}$	the crowding distance of i_sth solution in a nondominated set
Q	the optimal set in multi-objective optimization problem
S_τ	the set of solution that x_τ constrained dominates
V	the volume of reactor
c_1^i	the concentration of Fe^{2+} in $\#i$ reactor
c_2^i	the concentration of Fe^{3+} in $\#i$ reactor
c_3^i	the concentration of H^+ in $\#i$ reactor
$c_{0,1}^i$	the inlet concentration of Fe^{2+} in $\#i$ reactor
$c_{0,2}^i$	the inlet concentration of Fe^{3+} in $\#i$ reactor
$c_{0,3}^i$	the inlet concentration of H^+ in $\#i$ reactor
e^*	the evaluation value of fuzzy system
f_{if}	the i_fth objective function
g_{ig}	the i_gth inequality constraint function
i	the reactor number
i_f	the objective function number
i_g	the constraint function number
i_s	the solution number in a nondominated set
j	the solution number in an optimal set
k_1^i	the oxidation rate constant in $\#i$ reactor
k_2^i	the hydrolysis rate constant in $\#i$ reactor
k_3^i	the neutralization rate constant in $\#i$ reactor
l	the solution number in the state transition algorithm
m_τ	the number of solutions which constrained dominate x_τ
n	the control interval number
p_1	the price of oxygen
p_2	the price of zinc oxide
r_1^i	the oxidation rate in $\#i$ reactor
r_2^i	the hydrolysis rate in $\#i$ reactor
r_3^i	the neutralization rate in $\#i$ reactor
T_f	the final time of time span
u_1^i	the rate of the addition of oxygen in $\#i$ reactor
u_2^i	the rate of the addition of zinc oxide in $\#i$ reactor
v	the function of state and historical state
x	the candidate solution in the state transition algorithm

Acknowledgments

This study is supported by the National Natural Science Foundation of China (Grant No. 61503416 and No. 61533021), the 111 Project (Grant No. B17048), and the Foundation for Innovative Research Groups of the National Natural Science Foundation of China (Grant No. 61621062).

References

Angira, R., Santosh, A., 2007. Optimization of dynamic systems: a trigonometric differential evolution approach. Comput. Chem. Eng. 31, 1055–1063.
Balarini, J.C., Polli, L.D.O., Miranda, T.L.S., de Castro, R.M.Z., Salum, A., 2008. Importance of roasted sulphide concentrates characterization in the hydrometallurgical extraction of zinc. Miner. Eng. 21 (1), 100–110.
Bayat, M., Dehghani, Z., Rahimpour, M.R., 2014. Dynamic multi-objective optimization of industrial radial-flow fixed-bed reactor of heavy paraffin dehydrogenation in LAB plant using NSGA-II method. J. Taiwan Inst. Chem. Eng. 45, 1474–1484.
Chang, Y.F., Zhai, X.J., Li, B.C., Fu, Y., 2010. Removal of iron from acidic leach liquor of lateritic nickel ore by goethite precipitate. Hydrometallurgy 101 (1–2), 84–87.
Chen, W.L., Lu, X.W., Yao, C.H., 2015. Optimal strategies evaluated by multi-objective optimization method for improving the performance of a novel cycle operating activated sludge process. Chem. Eng. J. 260, 492–502.
Chen, X., Du, W.L., Qi, R., Qian, F., Tianfield, H., 2014a. Hybrid gradient particle swarm optimization for dynamic optimization problems of chemical processes. Asia Pac. J. Chem. Eng. 8 (5), 708–720.
Chen, X., Du, W.L., Qi, R., Tianfield, H., Qi, R.B., He, W.L., Qian, F., 2014b. Dynamic optimization of industrial processes with nonuniform discretization-based control vector parameterization. IEEE Trans. Autom. Sci. Eng. 11 (4), 1289–1299.
Deb, K., Agrawal, R.B., 1995. Simulated binary crossover for continuous search space. Complex Syst. 9 (3), 115–148.
Deb, K., Pratap, A., Agarwal, S., Meyarivan, T., 2002. A fast and elitist multiobjective genetic algorithm: NSGA-II. IEEE Trans. Evol. Comput. 6 (2), 182–197.
Farina, M., Deb, K., Amato, P., 2004. Dynamic multiobjective optimization problems: test cases, approximations and applications. IEEE Trans. Evol. Comput. 8 (5), 425–442.
Güler, E., Seyrankaya, A., 2016. Precipitation of impurity ions from zinc leach solutions with high iron contents - a special emphasis on cobalt precipitation. Hydrometallurgy 164, 118–124.
Han, J., Yang, C.H., Zhou, X.H., Gui, W.H., 2017a. A new multi-threshold image segmentation approach using state transition algorithm. Appl. Math. Model. 44, 588–601.
Han, J., Yang, C.H., Zhou, X.J., Gui, W.H., 2017b. A two-stage state transition algorithm for constrained engineering optimization problems. Int. J. Control. Autom. Syst (in press).
Helbig, M., Engelbrecht, A.P., 2013. Performance measures for dynamic multi-objective optimisation algorithms. Inf. Sci. 250, 61–81.
Ismael, M.R.C., Carvalho, J.M.R., 2003. Iron recovery from sulphate leach liquors in zinc hydrometallurgy. Miner. Eng. 16 (1), 31–39.
Kim, Y.H., Yoo, C.K., Lee, I.B., 2008. Optimization of biological nutrient removal in a SBR using simulation-based iterative dynamic programming. Chem. Eng. J. 13, 11–19.
Kong, W.J., Chai, T.Y., Yang, S.X., Ding, J.L., 2013. A hybrid evolutionary multiobjective optimization strategy for the dynamic power supply problem in magnesia grain manufacturing. Appl. Soft Comput. 13, 2960–2969.
Loan, M., Newman, O.M.G., Cooper, R.M.G., Farrow, J.B., Parkinson, G.M., 2006. Defining the paragoethite process for iron removal in zinc hydrometallurgy. Hydrometallurgy 81 (2), 104–129.
Na, J., Kshetrimayum, K.S., Lee, U., Han, C.H., 2016. Multi-objective optimization of microchannel reactor for Fischer-Tropsch synthesis using computational fluid dynamics and genetic algorithm. Chem. Eng. J. 313, 1521–1534.
Nazemi, M.K., Rashchi, F., Mostoufi, N., 2011. A new approach for identifying the rate controlling step applied to the leaching of nickel from spent catalyst. Int. J. Miner. Process. 100, 21–26.
Pappu, A., Saxena, M., Asolekar, S.R., 2006. Jarosite characteristics and its utilisation potentials. Sci. Total Environ. 529 (1–3), 232–243.
Peng, H., Zhang, Z., Wang, J., Shi, P., 2013. Audio watermarking framework using multi-objective particle swarm optimization. Int. J. Innov. Comput. Information and Control 9 (7), 2789–2800.
Pradel, J., Castillo, S., Traverse, J.P., Besset, R.G., Darcy, M., 1993. Ferric hydroxide oxide from the goethite process: characterization and potential use. Ind. Eng. Chem. Res. 32 (9), 1801–1804.
Riascos, C.A.M., Pinto, J.M., 2004. Optimal control of bioreactors: a simultaneous approach for complex systems. Chem. Eng. J. 99, 23–34.
Shi, P., 2002. Limit Hamilton-Jacobi-Isaacs equations for singularly perturbed zero-sum dynamic (discrete time) games. SIAM J. Control. Optim. 41 (3), 826–850.
Soroudi, A., Afrasiab, M., 2012. Binary PSO-based dynamic multi-objective model for distributed generation planning under uncertainty. IET Renew. Power Gneration 6 (2), 67–78.
Stumm, W., Lee, G.F., 1961. Oxygenation of ferrous iron. Ind. Eng. Chem. 53 (2), 143–146.
Takala, H., 1999. Leaching of zinc concentrates at Outokumpu Kokkola plant. erzmetall. 52 (1), 37–42.
Verbaan, B., Crundwell, F.K., 1986. An electrochemical model for the leaching of a sphalerite concentrate. Hydrometallurgy 16 (3), 345–359.
Wang, G.W., Yang, C.H., Zhu, H.Q., Li, Y.G., Peng, X.W., Gui, W.H., 2016. State-transition-algorithm-based resolution for overlapping linear sweep voltammetric peaks with high signal ratio. Chemom. Intell. Lab. Syst. 151, 61–70.
Wang, J., Peng, H., Shi, P., 2011. An optimal image watermarking approach based on multi-objective genetic algorithm. Inf. Sci. 181 (24), 5501–5524.
Xie, Y.F., Wei, S.M., Wang, X.L., Xie, S., Yang, C.H., 2016. A new prediction model based on the leaching rate kinetics in the alumina digestion process. Hydrometallurgy 164, 7–14.
Xie, Y.F., Xie, S.W., Chen, X.F., Gui, W.H., Yang, C.H., Caccetta, L., 2015a. An integrated predictive model with an on-line updating strategy for iron precipitation in zinc hydrometallurgy. Hydrometallurgy 151, 62–72.
Xie, S.W., Xie, Y.F., Li, Y.G., Yang, C.H., Gui, W.H., 2015b. Optimal control of oxidizing rate for iron precipitation process in zinc hydrometallurgy. ACTA Automat. Sin 41 (12).
Xie, Y.F., Xie, S.W., Li, Y.G., Yang, C.H., Gui, W.H., 2017. Dynamic modeling and optimal control of goethite process based on the rate-controlling step. Control. Eng. Pract. 58, 54–65.
Zhang, B., Yang, C.H., Zhu, H.Q., Li, Y.G., Gui, W.H., 2016. Evaluation strategy for the control of the copper removal process based on oxidation-reduction potential. Chem. Eng. J. 284, 294–304.
Zhou, X.J., Gao, D.Y., Yang, C.H., 2013. A comparative study of state transition algorithm with harmony search and artificial bee colony. Adv. Intell. Syst. Comput. 212, 651–659.
Zhou, X.J., Shi, P., Lim, C.C., Yang, C.H., Gui, W.H., 2017. A dynamic state transition algorithm with application to sensor network localization. Neurocomputing (in press).
Zhou, X.J., Yang, C.H., Gui, W.H., 2012. State transition algorithm. J. Ind. Manag. Optimization 8 (4), 1039–1056.
Zhou, X.J., Yang, C.H., Gui, W.H., 2014. Nonlinear system identification and control using state transition algorithm. Appl. Math. Comput. 226, 169–179.
Zhou, X.J., Yang, C.H., Gui, W.H., 2016. A Matlab toolbox for continuous state transition algorithm. Proc. 35th Chin. Control Conf. 9172–9177.